



## Stabilization of the platinum–ruthenium electrocatalyst against the dissolution of ruthenium with the incorporation of gold

Z.X. Liang, T.S. Zhao\*, J.B. Xu

Department of Mechanical Engineering, The Hong Kong University of Science and Technology, Clear Water Bay, Kowloon, Hong Kong SAR, China

### ARTICLE INFO

#### Article history:

Received 13 May 2008

Received in revised form 30 May 2008

Accepted 4 June 2008

Available online 13 June 2008

#### Keywords:

Direct methanol fuel cell (DMFC)

Methanol oxidation reaction

Polymer electrolyte membrane fuel cell (PEMFC)

Ruthenium crossover

Ruthenium dissolution

Stability

### ABSTRACT

The dissolution of Ru from the PtRu electrocatalyst has been identified as one of the most critical factors in degrading the performance of polymer electrolyte membrane fuel cells (PEMFC). In this work, we prepared an Au-modified PtRu catalyst (Au/PtRu) and found that the incorporation of Au could significantly stabilize the PtRu electrocatalyst against the dissolution of Ru. The X-ray photoelectron spectroscopy (XPS) characterization of the Au/PtRu catalysts revealed that the incorporation of Au increased the oxidation potential of Ru, which is the mechanism that leads to a reduction in the dissolution of Ru from the alloyed catalyst. The XPS characterization of the cathode catalyst also showed that with the PtRu as the anode catalyst Ru appeared at the cathode, but the crossover of Ru could be reduced when the anode catalyst was changed to Au/PtRu.

© 2008 Elsevier B.V. All rights reserved.

### 1. Introduction

Over the past decade, the polymer electrolyte membrane fuel cell (PEMFC) has been studied extensively as it shows a promise in stationary and mobile applications [1]. Although this type of fuel cell offers some important advantages, such as high power density and high energy-conversion efficiency, there are a number of challenging technical problems to be resolved before its widespread commercialization, in which the durability has been recognized as one of the most critical issues [2–7]. An irreversible loss of performance is generally encountered after a PEMFC operates for a certain time [2]. Although the mechanism leading to the performance loss has not been completely understood yet, the dissolution of platinum is believed to play a major role in degrading fuel cell performance [2,3,8,9]. Bindra et al. [8] studied the dissolution of Pt in phosphoric acid and found that the solubility increased with the potential up to 1.1 V. They further showed that the dissolution was a two-electron transfer reaction ( $\text{Pt} = \text{Pt}^{2+} + 2\text{e}^-$ ). This conclusion, however, is inconsistent with another recent work [10], in which Xu et al. studied the dissolution behavior of platinum in the acid media and found a ten-fold increase in the dissolved platinum concentration for every 92 mV increase in potential, which

is much less than the value of 29.5 mV per decade predicted for a two-electron dissolution reaction ( $\text{Pt} = \text{Pt}^{2+} + 2\text{e}^-$ ). Therefore, the dissolution of Pt may proceed in other mechanisms involving a series of one-electron-transfer reactions ( $\text{Pt-OH} = \text{Pt-OH}^+ + \text{e}^-$ ,  $\text{Pt-OH} + \text{H}^+ = \text{Pt}^{2+} + \text{H}_2\text{O} + \text{e}^-$ ) [2]. The dissolution can be explained by the calculation results with the density functional theory (DFT), which indicates that the one-electron-transfer reaction involving the electrochemical oxidation of oxyhydroxides is thermodynamically allowed [11]. Although the details of the mechanism are still controversial, it is widely accepted that the dissolution process is closely related to the electro-oxidation reaction and thereby affected by the electro-oxidation potential of platinum. With this understanding, increasing the electro-oxidation potential of platinum can be a way to reduce the dissolution of Pt. Most recently, Zhang et al. [12] found that the platinum nanoparticles could be stabilized against dissolution by depositing gold on the surface; the improved stability was achieved by the higher platinum oxidation potential resulted from the gold clusters.

Relatively, the studies of the stability problems of the anode catalyst are scarce. The PtRu alloy catalyst has been widely employed as the anode catalyst in PEMFC or direct methanol fuel cell (DMFC) due to its superior CO-tolerant ability [1,13]. Unfortunately, Ru is susceptible to leach out from the PtRu catalyst, which can also degrade fuel cell performance [14–17]. He et al. [14] found that the dissolution of Ru led to a continuous decrease in the anode activity of the PtRu catalyst to the methanol oxidation reaction (MOR) in phosphoric

\* Corresponding author. Tel.: +852 2358 8647.  
E-mail address: [metzhao@ust.hk](mailto:metzhao@ust.hk) (T.S. Zhao).

acid. Moreover, recent studies showed that the dissolution of Ru was also detrimental to the cathode performance of DMFCs [15–18]. Valdez et al. reported that Ru dissolved from the anode side would permeate through the polymer electrolyte membrane (PEM) and redeposit on the Pt nanoparticles at the cathode side, known as “Ru crossover” [15]. The deposition of Ru on the Pt sites could not only lower the activity to the oxygen reduction reaction (ORR) but also decrease its ability to handle “methanol crossover” [16]. The study by Piela et al. suggested that the overall effect of “Ru crossover” on the cell performance was from 40 mV up to 200 mV, depending on the degree of the cathode contamination [16].

Our literature review indicates that in addition to the dissolution of Pt at the cathode, the dissolution of Ru at the anode is also a critical issue, which can lead to fuel cell performance degradation. The objective of this work was to reduce the dissolution of Ru from the PtRu electrocatalyst by depositing the Au clusters onto the PtRu nanoparticles.

## 2. Experimental

Au was deposited onto the surface of the PtRu black catalyst (E-TEK Company) by a well-developed method [12,19–24]. The first step of this method is to form Cu monolayers onto the surface of the PtRu nanoparticles by the under-potential deposition (UPD) method. The prepared samples are then immersed into the  $\text{AuCl}_3$  solution so that the spontaneous deposition of Au will take place by the galvanic displacement of Cu monolayers. More specially, in this work, Cu was first deposited onto the PtRu catalyst with  $0.10 \text{ mol dm}^{-3} \text{ CuSO}_4$  solution (plus  $0.50 \text{ mol dm}^{-3} \text{ H}_2\text{SO}_4$ ). The PtRu catalyst covered with Cu monolayers was rinsed to remove residual  $\text{CuSO}_4$ , and placed into  $1.0 \text{ mmol dm}^{-3} \text{ AuCl}_3$  solution in an  $\text{N}_2$  atmosphere. After the immersion for ten minutes, Cu was completely displaced by Au; the electrode was then immersed in  $0.50 \text{ mol dm}^{-3} \text{ H}_2\text{SO}_4$  solution to exchange the metal ions for another ten minutes. Finally, the electrode was rinsed in D.I. water to remove the absorbed sulfuric acid.

The electrochemical characterizations of the prepared catalyst samples were conducted in a fuel cell setup [4], in which the PtRu catalyst or the Au/PtRu catalyst was used at the anode, while the Pt catalyst was employed at the cathode. A Nafion® 115 membrane, pretreated according to the standard procedures detailed elsewhere [25–27], was used as the electrolyte. The experiments were carried out by connecting, respectively, the anode of the cell to the working electrode and the cathode to the reference and counter electrodes of a potentiostat.

The dissolution of Ru from the PtRu and the Au/PtRu catalysts was studied using the potential cycling technique [2,16–18]. During the course of the experiments, the anode was fed with D.I. water (deaerated by ultrahigh purity nitrogen for 30 min) at the flow rate of  $1.0 \text{ ml min}^{-1}$ , while the cathode was fed with the hydrogen gas at  $20.0 \text{ ml min}^{-1}$  (serving as the dynamic hydrogen electrode, DHE). The potential of the anode was swept from  $0.20 \text{ V}$  to  $0.80 \text{ V}$  (vs. DHE) at the scanning rate of  $0.20 \text{ V s}^{-1}$ . The degradation behavior of the electrocatalysts after various cycles of potential cycling was characterized by the anode polarization curve and the methanol stripping curve [17,18].

The anode polarization curve was measured by feeding hydrogen to the cathode at  $20 \text{ ml min}^{-1}$  and methanol solution ( $1.0 \text{ mol dm}^{-3}$ ) to the anode at  $1.0 \text{ ml min}^{-1}$ . The anode polarization curve was recorded by applying the potential between  $0 \text{ V}$  and  $0.40 \text{ V}$  with a scanning rate of  $3 \text{ mV s}^{-1}$ . Methanol stripping method was used to measure the active surface area of the PtRu catalyst [28]. Methanol was first adsorbed onto the PtRu catalyst by flowing  $1.0 \text{ mol dm}^{-3}$  methanol solution through the anode for 20 min,

while holding the PtRu catalyst electrode potential at  $0.10 \text{ V}$  (vs. DHE). The anode was then washed by flowing D.I. water through the electrode for 10 min, while the potential was still held at  $0.10 \text{ V}$ , to remove methanol from the anode chamber. The methanol stripping curve was recorded in the potential range between  $0.10 \text{ V}$  and  $0.70 \text{ V}$  at  $20 \text{ mV s}^{-1}$ .

## 3. Results and discussion

Fig. 1 shows the cyclic voltammogram of the PtRu catalyst in  $0.10 \text{ mol dm}^{-3} \text{ CuSO}_4$  plus  $0.50 \text{ mol dm}^{-3} \text{ H}_2\text{SO}_4$  aqueous solution. For comparison, the voltammogram in the base electrolyte is also shown in the same figure. In the case of the forward scan, the hydrogen desorption region ( $-0.2$ – $0 \text{ V}$  vs. saturated calomel electrode, SCE) is masked in the presence of copper, and two more peaks (centered at  $0.1 \text{ V}$  and  $0.5 \text{ V}$ ) corresponding to the Cu stripping are present. As to the backward scan, the oxide reduction peak is distorted by the onset of Cu UPD, of which the peak is around  $0.1 \text{ V}$ . This result is consistent with that reported previously [29,30]. Kucernak and Green [29,30] attributed the peak at lower potential to the copper deposition on ruthenium sites, while the other peak at higher potential to the deposition on platinum sites in the bimetallic PtRu catalyst. They further demonstrated that Cu monolayers could be uniformly deposited onto both Pt and Ru sites below the UPD potential of  $0.3 \text{ V}$ . When the potential exceeded  $0.3 \text{ V}$ , ruthenium would be oxidized gradually; as a result, the deposition of Cu on Ru sites would be hindered and only occur on Pt sites. For this reason, the deposition potential in this work was selected to be  $0.30 \text{ V}$  (vs. standard hydrogen electrode, SHE) for the uniform deposition of Cu monolayers, which ensured further uniform deposition of Au onto the PtRu catalyst.

It is well understood that pure Au is inactive to the methanol oxidation reaction in acid electrolyte at low temperatures. The deposited Au can occupy the active sites of the PtRu catalyst, which might reduce its electrocatalytic activity to the MOR. Therefore, we need to study the effect of the Au deposition on the electrocatalytic activity of the catalyst. Fig. 2 shows the anode polarization curves of the PtRu catalyst and the Au/PtRu catalyst. The anode polarization curve of the Au/PtRu catalyst is found to be slightly better than that of the PtRu catalyst, indicating that the deposition of Au can promote the kinetics of the MOR. The improvement was also reported elsewhere, and was generally attributed to the synergistic effect between Au and Pt or PtRu [31–40]. Au is a highly active catalyst to catalyze CO oxidation reaction at low temperatures [41]. And

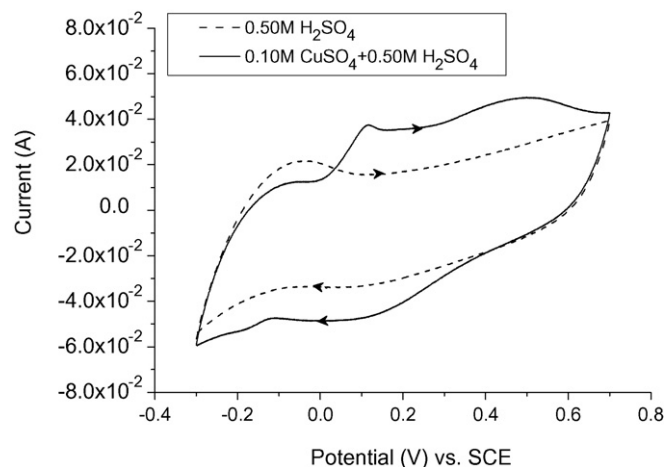


Fig. 1. Cyclic voltammograms of the PtRu catalyst in  $0.50 \text{ mol dm}^{-3} \text{ H}_2\text{SO}_4$  and  $0.10 \text{ mol dm}^{-3} \text{ CuSO}_4$  plus  $0.50 \text{ mol dm}^{-3} \text{ H}_2\text{SO}_4$ .

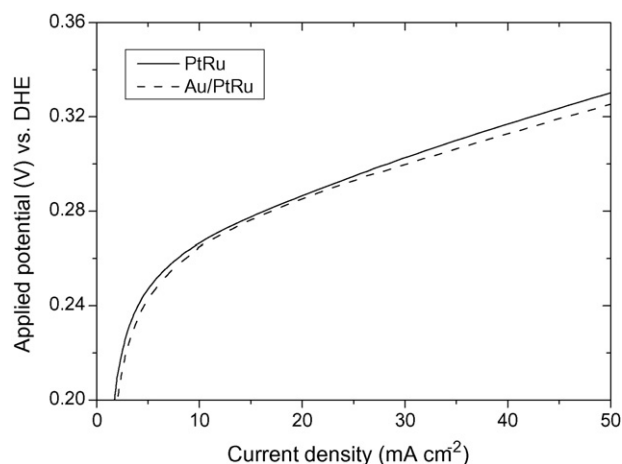
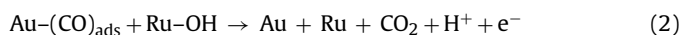
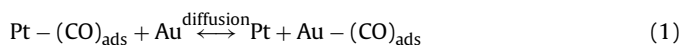


Fig. 2. Anode polarization curves of the PtRu catalyst and the Au/PtRu catalyst.

the incorporation of Au to Pt based catalyst can effectively reduce the overpotential of the CO oxidation reaction [31–34]. Based on this information, the CO-like species formed on Pt sites during the MOR may ‘jump’ to the neighboring Au sites and then be electro-oxidized by the oxygen-containing species on Ru sites [34,35]. The latter reaction can be carried out without activation energy, which may be the mechanism that lowers the overpotential of the MOR on the Au/PtRu catalyst. The synergistic effect can be described as:



We now need to consider the possibility of the CO diffusion, Eq. (1), to rationalize the above analysis. Firstly, the CO diffusion on the Pt catalyst has been reported to be an important process that considerably affects the CO oxidation reaction [42,43]. A rough estimation shows that a single adsorbed CO molecule can make over  $10^5$  jumps between nearest adsorption sites during the time interval of 100 s. Therefore, the CO diffusion at the interface between Au and Pt is possible. Secondly, the adsorption energy of CO on Pt(111) and Au(100) was reported to be  $85 \text{ kJ mol}^{-1}$  and  $58 \text{ kJ mol}^{-1}$ , respectively [44,45]. The energy change for the CO diffusion between the Pt sites and the Au sites can thus be estimated to be around  $30 \text{ kJ mol}^{-1}$ , which is not a large value. Accordingly, it is reasonable to suppose that the CO diffusion, Eq. (1), occurs quasi-reversibly at the Au/Pt interface and facilitates the successive  $(\text{CO})_{\text{ads}}$  removal reaction, Eq. (2). In summary, the synergistic effect between Au and PtRu can enhance the electrocatalytic activity toward the MOR with the Au/PtRu catalyst.

Fig. 3 shows the change of the anode polarization curves of the PtRu catalyst and the Au/PtRu catalyst during the course of the potential cycling. From Fig. 3a, it can be seen that the anode overpotential of the PtRu catalyst increased by 20 mV after 10,000 cycles of potential cycling. In contrast, however, the anode polarization curve of the Au/PtRu catalyst exhibit negligible changes during the potential cycling test, as seen from Fig. 3b. Hence, it can be concluded that the electrochemical stability of the Au/PtRu catalyst is higher than the original PtRu catalyst. The higher electrochemical stability of the Au/PtRu catalyst can also be observed from the methanol stripping results shown in Fig. 4. As can be seen from Fig. 4a, for the PtRu catalyst, the peak potential of the methanol stripping curve shifted to higher potentials after potential cycling. For the Au/PtRu catalyst, however, Fig. 4b indicates that the peak potential did not change. The positive shift in the peak potentials has been regarded as the indication of the dissolution of Ru from

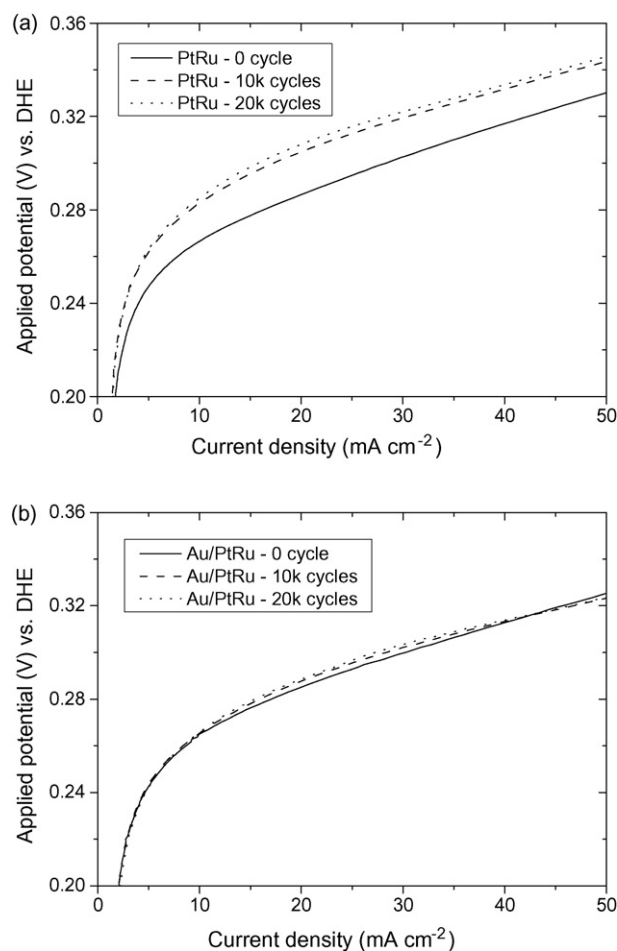
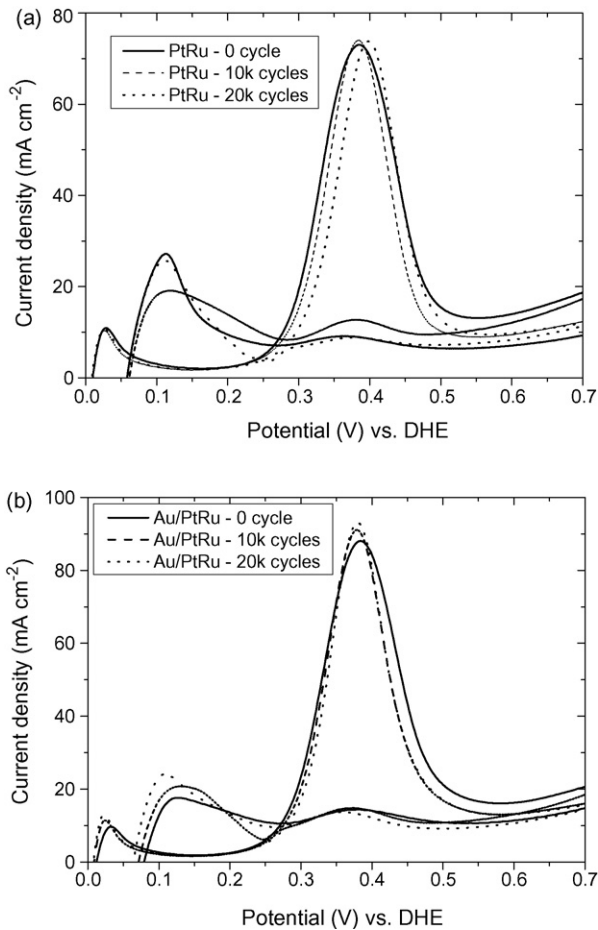


Fig. 3. The change of the anode polarization curves of the PtRu catalyst and the Au/PtRu catalyst during the course of potential cycling: (a) the PtRu catalyst and (b) the Au/PtRu catalyst.

the PtRu catalyst [16–18]. In summary, both the anode polarization and methanol stripping results shown in Figs. 3 and 4 indicate that Ru is inclined to leach out from the PtRu catalyst, but the incorporation of Au into the catalyst can significantly stabilize the PtRu catalyst against the dissolution of Ru.

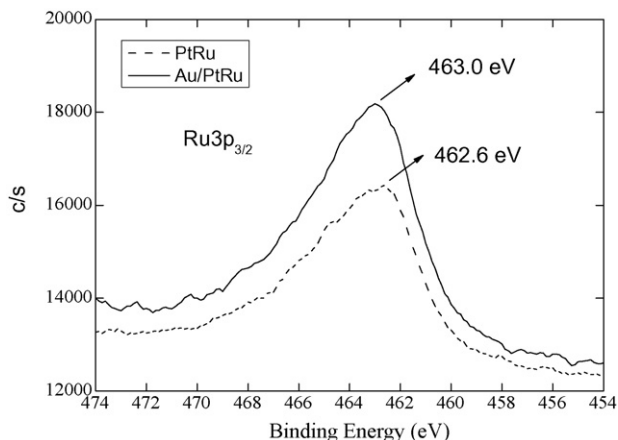
To study the mechanism why the incorporation of Au into the PtRu catalyst can stabilize the PtRu catalyst, we characterized the change in the elemental electronic structure of Ru before and after the incorporation of Au using X-ray photoelectron spectroscopy (XPS). The XPS spectra of Ru  $3p_{3/2}$  of the PtRu catalyst and the Au/PtRu catalyst are compared in Fig. 5. A positive shift of 0.4 eV is seen in the binding energy of Ru  $3p_{3/2}$  after the incorporation of Au, indicating that the electronic structure of Ru was altered and a charge transfer flew from Ru to Au. This result is consistent with that by Kuhn et al. [46], who investigated the electronic properties of the Au/Ru(001) surfaces and found a net charge transfer from Ru toward Au based on the ab initio self-consistent-field calculations. As the electron loss in Ru increases the oxidation state of Ru, the oxidation of Ru ( $\text{Ru} = \text{Ru}^{3+} + 3\text{e}^-$ ) in the Au/PtRu catalyst requires much higher potentials than in the unmodified one. As a result, the dissolution of Ru can be reduced and the PtRu catalyst can be stabilized by the incorporation of Au [12].

Fig. 6 shows the XPS spectra of Ru3p and Pt4f of the cathode catalyst with the PtRu catalyst and the Au/PtRu catalyst as the anode catalysts after potential cycling for 20,000 cycles. From Fig. 6a, it can be observed that the peak of Ru3p was very clear for the cath-



**Fig. 4.** The change of the methanol stripping curves of the PtRu catalyst and the Au/PtRu catalyst during the course of potential cycling: (a) the PtRu catalyst and (b) the Au/PtRu catalyst.

ode catalyst with the PtRu catalyst as the anode catalyst; however, the signal of Ru3p was rather weak for the cathode catalyst with the Au/PtRu catalyst as the anode catalyst, as shown in Fig. 6b. This indicates that considerable amount of Ru was present in the cathode catalyst with the PtRu as the anode catalyst, whereas only traces of Ru existed in the cathode catalyst with the Au/PtRu as the anode catalyst. The presence of element Ru in the cathode catalyst stems from the crossover of Ru from the anode to the cathode, as



**Fig. 5.** XPS spectra of Ru  $3p_{3/2}$  of the PtRu catalyst and the Au/PtRu catalyst.

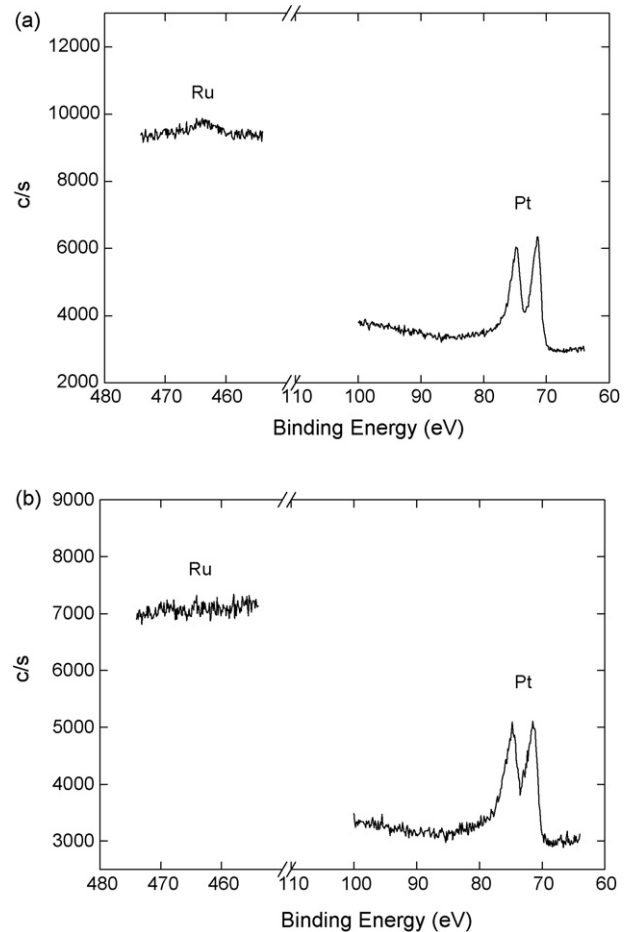


**Fig. 6.** XPS spectra of Ru 3p and Pt 4f of the cathode catalyst with the PtRu and the Au/PtRu as the anode catalyst after potential cycling for 20,000 cycles: (a) the PtRu catalyst and (b) the Au/PtRu catalyst.

reported previously [15,16]. With the PtRu as the anode catalyst, Ru, which leached out during the potential cycling test, could permeate through the polymer electrolyte membrane and redeposit onto the surface of the Pt catalyst in the cathode, resulting in a considerable amount of Ru in the cathode catalyst. In contrast, the dissolution of Ru was significantly suppressed for the Au/PtRu catalyst; as a result, the crossover of Ru was reduced to a great extent. This explains why only trace amount of Ru was found in the cathode catalyst with the Au/PtRu as the anode catalyst.

#### 4. Conclusions

In this work, we demonstrated that the stability of the PtRu catalyst was significantly improved against the dissolution of Ru as a result of the incorporation of Au. The XPS characterization of the Au/PtRu catalysts revealed that the incorporation of Au increased the oxidation potential of Ru, which is the mechanism that leads to a reduction in the dissolution of Ru from the alloyed catalyst. Furthermore, we found that the crossover of Ru could be reduced when the Au/PtRu catalyst was employed as the anode catalyst.

#### Acknowledgements

The work described in this paper was supported by a grant from the Research Grants Council of the Hong Kong Special Administrative Region, China (Project No. 622807).

## References

- [1] A.S. Arico, S. Srinivasan, V. Antonucci, *Fuel Cells* 1 (2001) 133–161.
- [2] R. Borup, J. Meyers, B. Pivovar, Y.S. Kim, R. Mukundan, N. Garland, D. Myers, M. Wilson, F. Garzon, D. Wood, P. Zelenay, K. More, K. Stroh, T. Zawodzinski, J. Boncella, J.E. McGrath, M. Inaba, K. Miyatake, M. Hori, K. Ota, Z. Ogumi, S. Miyata, A. Nishikata, Z. Siroma, Y. Uchimoto, K. Yasuda, K.I. Kimijima, N. Iwashita, *Chem. Rev.* 107 (2007) 3904–3951.
- [3] J. Xie, D.L. Wood, D.M. Wayne, T.A. Zawodzinski, P. Atanassov, R.L. Borup, *J. Electrochem. Soc.* 152 (2005) A104–A113.
- [4] Z.X. Liang, T.S. Zhao, J. Prabhuram, *Electrochim. Acta* 51 (2006) 6412–6418.
- [5] J.G. Liu, Z.H. Zhou, X.X. Zhao, Q. Xin, G.Q. Sun, B.L. Yi, *Phys. Chem. Chem. Phys.* 6 (2004) 134–137.
- [6] T. Tanuma, S. Terazono, *Chem. Lett.* 35 (2006) 1422–1423.
- [7] J.R. Yu, T. Matsuura, Y. Yoshikawa, M.N. Islam, M. Hori, *Phys. Chem. Chem. Phys.* 7 (2005) 373–378.
- [8] P. Bindra, S.J. Clouser, E. Yeager, *J. Electrochem. Soc.* 126 (1979) 1631–1632.
- [9] T. Tada, N. Tushima, Y. Yamamoto, M. Inoue, *Electrochemistry* 75 (2007) 221–230.
- [10] X.P. Wang, R. Kumar, D.J. Myers, *Electrochem. Solid State Lett.* 9 (2006) A225–A227.
- [11] Z.H. Gu, P.B. Balbuena, *J. Phys. Chem. A* 110 (2006) 9783–9787.
- [12] J. Zhang, K. Sasaki, E. Sutter, R.R. Adzic, *Science* 315 (2007) 220–222.
- [13] K. Koczkur, Q.F. Yi, A.C. Chen, *Adv. Mater.* 19 (2007) 2648–2652.
- [14] C.Z. He, H.R. Kunz, J.M. Fenton, *J. Electrochem. Soc.* 144 (1997) 970–979.
- [15] T.I. Valdez, S. Firdosy, B.E. Koel, S.R. Narayanan, *ECS Trans.* 1 (2006) 293–303.
- [16] P. Piela, C. Eickes, E. Broscha, F. Garzon, P. Zelenay, *J. Electrochem. Soc.* 151 (2004) A2053–A2059.
- [17] W.M. Chen, G.Q. Sun, J.S. Guo, X.S. Zhao, S.Y. Yan, J. Tian, S.H. Tang, Z.H. Zhou, Q. Xin, *Electrochim. Acta* 51 (2006) 2391–2399.
- [18] W.M. Chen, G.Q. Sun, Z.X. Liang, Q. Mao, H.Q. Li, G.X. Wang, Q. Xin, H. Chang, C.H. Pak, D.Y. Seung, *J. Power Sources* 160 (2006) 933–939.
- [19] J. Zhang, Y. Mo, M.B. Vukmirovic, R. Klie, K. Sasaki, R.R. Adzic, *J. Phys. Chem. B* 108 (2004) 10955–10964.
- [20] J. Zhang, F.H.B. Lima, M.H. Shao, K. Sasaki, J.X. Wang, J. Hanson, R.R. Adzic, *J. Phys. Chem. B* 109 (2005) 22701–22704.
- [21] M.H. Shao, T. Huang, P. Liu, J. Zhang, K. Sasaki, M.B. Vukmirovic, R.R. Adzic, *Langmuir* 22 (2006) 10409–10415.
- [22] M.B. Vukmirovic, J. Zhang, K. Sasaki, A.U. Nilekar, F. Uribe, M. Mavrikakis, R.R. Adzic, *Electrochim. Acta* 52 (2007) 2257–2263.
- [23] R.R. Adzic, J. Zhang, K. Sasaki, M.B. Vukmirovic, M. Shao, J.X. Wang, A.U. Nilekar, M. Mavrikakis, J.A. Valerio, F. Uribe, *Top. Catal.* 46 (2007) 249–262.
- [24] F.H.B. Lima, J. Zhang, M.H. Shao, K. Sasaki, M.B. Vukmirovic, E.A. Ticianelli, R.R. Adzic, *J. Phys. Chem. C* 111 (2007) 404–410.
- [25] Z.X. Liang, T.S. Zhao, J. Prabhuram, *J. Membr. Sci.* 283 (2006) 219–224.
- [26] Z.X. Liang, T.S. Zhao, C. Xu, J.B. Xu, *Electrochim. Acta* 53 (2007) 894–902.
- [27] Z.X. Liang, T.S. Zhao, *J. Phys. Chem. C* 111 (2007) 8128–8134.
- [28] X.S. Zhao, G.Q. Sun, L.H. Jiang, W.M. Chen, S.H. Tang, B. Zhou, Q. Xin, *Electrochem. Solid State Lett.* 8 (2005) A149–A151.
- [29] C.L. Green, A. Kucernak, *J. Phys. Chem. B* 106 (2002) 1036–1047.
- [30] C.L. Green, A. Kucernak, *J. Phys. Chem. B* 106 (2002) 11446–11456.
- [31] J.H. Choi, K.W. Park, I.S. Park, K. Kim, J.S. Lee, Y.E. Sung, *J. Electrochem. Soc.* 153 (2006) A1812–A1817.
- [32] J.H. Zeng, J. Yang, J.Y. Lee, W.J. Zhou, *J. Phys. Chem. B* 110 (2006) 24606–24611.
- [33] J.B. Xu, T.S. Zhao, Z.X. Liang, L.D. Zhu, *Chem. Mater.* 20 (2008) 1688–1690.
- [34] K. Matsuoka, K. Miyazaki, Y. Iriyama, K. Kikuchi, T. Abe, Z. Ogumi, *J. Phys. Chem. C* 111 (2007) 3171–3174.
- [35] H.J. Kim, D.Y. Kim, H. Han, Y.G. Shul, *J. Power Sources* 159 (2006) 484–490.
- [36] X.B. Ge, R.Y. Wang, P.P. Liu, Y. Ding, *Chem. Mater.* 19 (2007) 5827–5829.
- [37] J. Luo, P.N. Njoki, Y. Lin, D. Mott, L.Y. Wang, C.J. Zhong, *Langmuir* 22 (2006) 2892–2898.
- [38] Y.B. Lou, M.M. Maye, L. Han, J. Luo, C.J. Zhong, *Chem. Commun.* (2001) 473–474.
- [39] S. Kumar, S.Z. Zou, *Langmuir* 23 (2007) 7365–7371.
- [40] H.P. Liang, T.G. Jones, N.S. Lawrence, L. Jiang, J.S. Barnard, *J. Phys. Chem. C* 112 (2008) 4327–4332.
- [41] M.C. Kung, R.J. Davis, H.H. Kung, *J. Phys. Chem. C* 111 (2007) 11767–11775.
- [42] A.V. Petukhov, W. Akemann, K.A. Friedrich, U. Stimming, *Surf. Sci.* 404 (1998) 182–186.
- [43] T. Kobayashi, P.K. Babu, J.H. Chung, E. Oldfield, A. Wieckowski, *J. Phys. Chem. C* 111 (2007) 7078–7083.
- [44] G. Ertl, M. Neumann, K.M. Streit, *Surf. Sci.* 64 (1977) 393–410.
- [45] G. Mcelhiney, J. Pritchard, *Surf. Sci.* 60 (1976) 397–410.
- [46] M. Kuhn, J.A. Rodriguez, J. Hrbek, A. Bzowski, T.K. Sham, *Surf. Sci.* 341 (1995) L1011–L1018.